ISSN 0036-0236, Russian Journal of Inorganic Chemistry, 2016, Vol. 61, No. 12, pp. 1505–1511. © Pleiades Publishing, Ltd., 2016.
Original Russian Text © N.P. Simonenko, V.A. Nikolaev, E.P. Simonenko, N.B. Generalova, V.G. Sevastyanov, N.T. Kuznetsov, 2016, published in Zhurnal Neorganicheskoi Khimii, 2016, Vol. 61, No. 12, pp. 1566–1572.

SYNTHESIS AND PROPERTIES OF INORGANIC COMPOUNDS

Preparation of Nanostructured Titania Thin Films by Sol–Gel Technology

N. P. Simonenko[a, *], V. A. Nikolaev[a], E. P. Simonenko[a, b], N. B. Generalova[a], V. G. Sevastyanov[a], and N. T. Kuznetsov[a, b]

[a] *Kurnakov Institute of General and Inorganic Chemistry, Russian Academy of Sciences, Leninskii pr. 31, Moscow, 119991 Russia*

[b] *Samara State Aerospace University (National Research University), Samara, Russia*

**e-mail: n_simonenko@mail.ru*

Received May 29, 2016

Abstract—This study is concerned with the preparation of hydrolytically active heteroligand complex $[Ti(OC_4H_9)_{3.61}(O_2C_5H_7)_{0.39}]$ from titanium butoxide and acetylacetone and with the gel formation kinetics in a solution of this complex upon hydrolysis and polycondensation. Single-layer and double-layer thin films of a solution of this precursor were coated on polished silicon substrates using the dip-coating method. The crystallization of nanostructured titania films during the heat treatment of these xerogel coatings was studied using various protocols; the anatase–rutile phase transition temperature was found to depend on the film thickness. The effects of the precursor solution viscosity on the film thickness and crystallite size were determined.

DOI: 10.1134/S0036023616120184

Titania is known to have a unique set of useful properties (chemical stability, biocompatibility, useful physical, optical and electrical characteristics). For this reason, titania is in great demand and is a well-characterized material. Titania-based materials are primarily demanded in a search for alternative energy sources [1, 2] and in photocatalyst design [3–9]; they are also prospective materials for optical devices [10]. Thin-film materials are increasingly required to improve the efficiency of products. Sol–gel technology, where precursors are hydrolytically active heteroligand complexes, offers one of the most promising and convenient approaches to preparation of diverse types of nanomaterials. This is a universal method for preparing metal oxides in the form of powders [11–14], nanostructured thin films [15–18], microtubes [19], and composite matrices [20], on one hand, and refractory carbides [21–23], on the other. The advantage of this approach consists of control over the rheology of precursor solutions and the kinetics of their alteration upon hydrolysis, the factors that determine the functional characteristics of products to a considerable degree.

Therefore, our goals were as follows: to study the preparation of hydrolytically active heteroligand complexes $[Ti(OC_4H_9)_{3.61}(O_2C_5H_7)_{0.39}]$, to determine how the rheology of their solutions influences the properties of thin nanostructured titania films, to elucidate the dependence of the anatase–rutile phase transition temperature on the oxide coating thickness, and to study the microstructural evolution of the oxide film as a result of this phase transition.

EXPERIMENTAL

The reagents used were titanium butoxide $Ti(OC_4H_9)_4$ (Sigma-Aldrich, reagent grade, 97%), acetylacetone $C_5H_8O_2$ (pure grade), *n*-butanol $C_4H_{10}O$ (specialty grade), and ethanol C_2H_6O (fractionally distilled).

Solutions of hydrolytically active heteroligand complexes of composition $[Ti(OC_4H_9)_{3.61}(O_2C_5H_7)_{0.39}]$ were prepared as described earlier [12]: to titanium butoxide, acetylacetone was added in a required amount under stirring for chelating moieties to substitute for alkoxy groups. This was performed to increase the shielding of titanium(IV) cations and reduce the reactivity of the complexes in subsequent reaction with water. Afterwards, the reaction systems were reduced in volume to 50 mL, the solvent (1-butanol) was added, and then a hydrolyzing agent (a solution of water in ethanol; $\varphi(H_2O)$ = 50%) was added drop-by-drop under stirring. After all components were stirred for 1.5 min, the spindle L2 of a Fungilab Smart L rotary viscometer (the shear speed was 100 rpm) was immersed into the solution to start measurements of dynamic viscosity η. When a certain η value was reached, thin solution films were applied

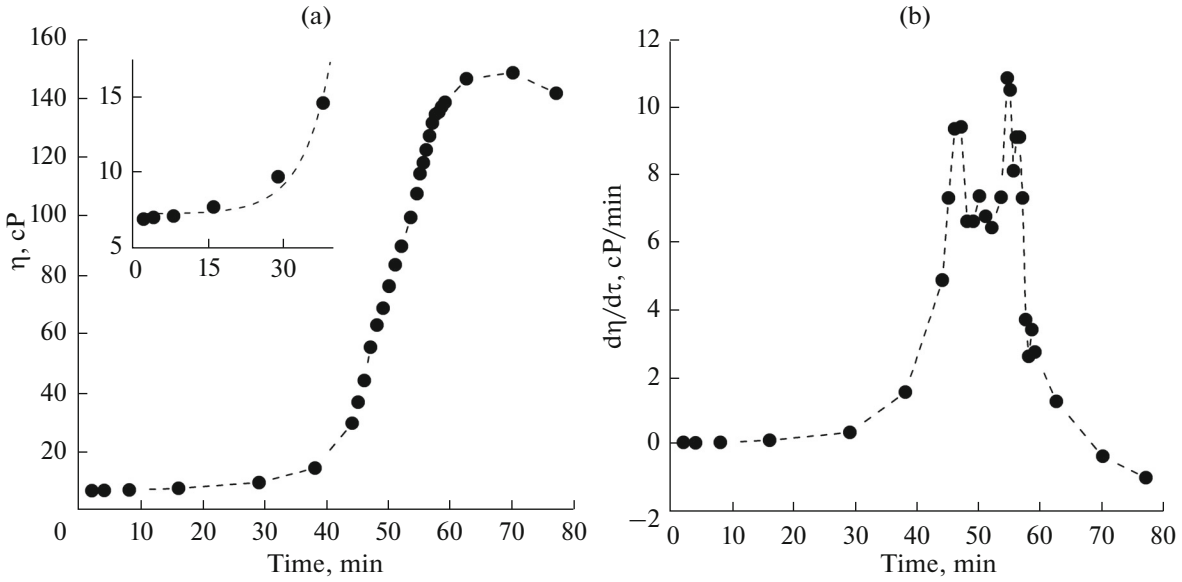

Fig. 1. (a) Dynamic viscosity curve for a $[Ti(OC_4H_9)_{3.61}(O_2C_5H_7)_{0.39}]$ solution during hydrolysis and polycondensation and (b) its derivative curve.

to the surfaces of polished single-crystalline silica substrates by the dip-coating method (the withdrawal speed was 1 mm/s). Then, hydrolysis and polycondensation in the film bulk proceeded to yield a three-dimensional network. This was followed by 60-min exposure of the samples under air at 25°C to complete the xerogel coating formation. Some samples were coated with a second layer by the same protocol. Subsequently, the samples were heat-treated at various temperatures for 1 h under air to crystallize titania thin films.

X-ray diffraction patterns were recorded from surfaces of oxide films on a D8 Advance (Bruker) X-ray diffractometer in a characteristic 2θ range of 24°–28° (Ni-filtered Cu$K_{\alpha 1}$ radiation, $E = 40$ keV, $I = 40$ mA, $t = 2.0$ s per point, 0.02° steps).

The microstructure of oxide films were studied using an NVision 40 (Carl Zeiss) three-beam workstation equipped with an EDX Oxford Instruments energy-dispersive analysis unit, and using a Solver Pro-M (NT-MDT) scanning probe microscope.

The adhesion of films was studied by a standard V-notch test using an Elcometer 107 adhesion meter.

RESULTS AND DISCUSSION

Synthesis of $[Ti(OC_4H_9)_{3.61}(O_2C_5H_7)_{0.39}]$ Complexes and Studies of Their Hydrolysis and Polycondensation

Addition of the required amount of acetylacetone and *n*-butanol as solvent to titanium butoxide produced a solution of complexes $[Ti(OC_4H_9)_{3.61}(O_2C_5H_7)_{0.39}]$ ($c = 0.25$ mol/L), which were less hydrolytically active. Previous studies showed that this coordination sphere composition and this precursor concentration were optimal, in the context of reactivity, for preparing thin films. So, addition of a hydrolyzing agent (a solution of water in ethanol, $\varphi(H_2O) = 50\%$) to the thus-prepared titanium alkoxoacetylacetonate solution (50 mL), initiated hydrolysis and polycondensation, which were accompanied with a rise in dynamic viscosity (Fig. 1). Figure 1 implies that the formation of a three-dimensional network is a multistep process. Following water addition, the dynamic viscosity experiences an exponential rise for 45 min to reach a gelation rate of about 9.5 cP/min. This is followed by a reduction in gel-formation rate and its stabilization at a level of 7 cP/min. The next step is observed in the 53th minute with an attendant abrupt rise in gelation rate to 11 cP/min, which is then followed by an exponential decline in gelation rate to zero (the dynamic viscosity reaches its maximal value of ~150 cP). Then, the viscosity of the system starts to decrease and, accordingly, the gelation rate acquires a negative value.

Crystallization of Titania Thin Films

After hydrolysis and polycondensation were studied, polished single-crystalline silicon substrates were coated with thin films of a precursor solution by dip coating at various dynamic viscosity values (7.5, 9.0, 10.5, and 12.0 cP). After the end of hydrolysis and polycondensation in the film bulk, a three-dimensional network was formed. Then, the samples were exposed to air for 60 min at 25°C to complete gel syneresis and xerogel film formation. Some samples were coated with a second layer by the same protocol.

Average crystallite sizes L_{101} (anatase) and L_{110} (rutile) in titania thin films prepared at various temepratures (nm)

T, °C	1 layer (7.5 cP)		2 layers (7.5 cP)		1 layer (9 cP)	1 layer (10.5 cP)	1 layer (12 cP)
	anatase	rutile	anatase	rutile	anatase		
400	9		18				
500	9		21		19	21	24
600	25		29		28	32	29
700	22		40		30	30	39
800	20		53	56	31	38	39
900	35		43	46			
1000	40			47			
1100	40	41		47			
1200	45	53		64			

The samples were heat-treated at various temperatures (400–1200°C in 100°C steps) under air for 1 h to study the crystallization of titania thin films. The X-ray powder diffraction was used to study the surface crystal structure of the coatings (Fig. 2). X-ray diffraction patterns imply the following. In single-layer films (whose thickness was ~50 nm as probed by microscopy), the clear-cut anatase structure was observed starting at 600°C. A minor rutile phase became noticeable starting at 900°C, which is 200°C higher than the anatase–rutile phase transition temperature in powders [12]. The rutile phase fraction increased as temperature rose, and the anatase phase survived in noticeable amounts up to 1200°C, which is of special interest. In the production of double-layer titania thin films (whose thickness was ~100 nm as probed by microscopy), the situation was appreciable different: a crystalline anatase phase was formed in noticeable amounts at 400°C, and a minor rutile phase appeared at 600–700°C. At 1000°C, transformation to the rutile structure was complete. Evidently, the thermal behavior of double-layer xerogel films resembled very much the behavior of powders. Thus, we showed that the increasing film thicknesses promote titania crystallization and appreciably reduce the anatase–rutile phase transition temperature.

The heat treatment of thin xerogel films prepared with precursor solutions of various viscosities at temperatures in the range 500–800°C in all cases yielded to anatase titania films. Small rutile admixtures were observed only in two samples (7.5 cP, 800°C; and 9.0 cP, 700°C), which could be due to insignificant defects generated in the films during application. X-ray diffraction patterns imply that the oxide films formed at higher precursor solution viscosities features stronger reflections, which is circumstantial evidence of their increased thicknesses. The average crystallite size increased in association (table). The average crystallite sizes of anatase for double-layer films were appreciably greater than for single-layer films, and the anatase–rutile phase transition was observed when the anatase crystallite size reached 40–50 nm. Thus, we may assume that the phase transition in single-layer films is hindered by an insufficient amount of the material required for crystallite growth along the axis normal to the substrate surface.

The microstructure of the prepared titania thin films was studied using scanning electron microscopy (SEM). The micrographs (Fig. 3) show that compact structures with poorly pronounced texture were formed at 400–600°C. A rise in temperature to 700–900°C gave rise to the formation of nanostructured films with particle sizes of ~30 nm, which agrees with an estimate of the average crystallite size; that is, a titania particle in this case, as a rule, consisted of a single crystallite. As temperature rose within this range, pores with sizes of ~30 nm also appeared. At 1000°C, the particles had an average size of ~40 nm. On the substrate edges, where defects can appear in the form of cracks and exfoliations due to an excessive thickness of the precursor solution film, there was a microstructure dimension gradient: particle sizes increased systematically in the direction to the defect. Thus, we can assume that a thicker xerogel film was formed in the region of the defect, which gave rise to the anatase–rutile phase transition in this region, accompanied by a sharp change in the coating microstructure. The contribution from these peripheral substrate regions was likely to manifest itself in the appearance of a low-intensity rutile reflection in the X-ray diffraction pattern. A rise in temperature to 1100°C led to further transformation of the film microstructure. The particle size distribution was bimodal: about 60% of the particles having an average size of ~40 nm were uniformly distributed in between larger particles (100–150 nm). The results of X-ray powder diffraction (the intensity ratio of anatase and rutile reflections) imply that the small particles had anatase structure and the larger ones had rutile structure. A rise in temperature to 1200°C continued the evolution of surface micro-

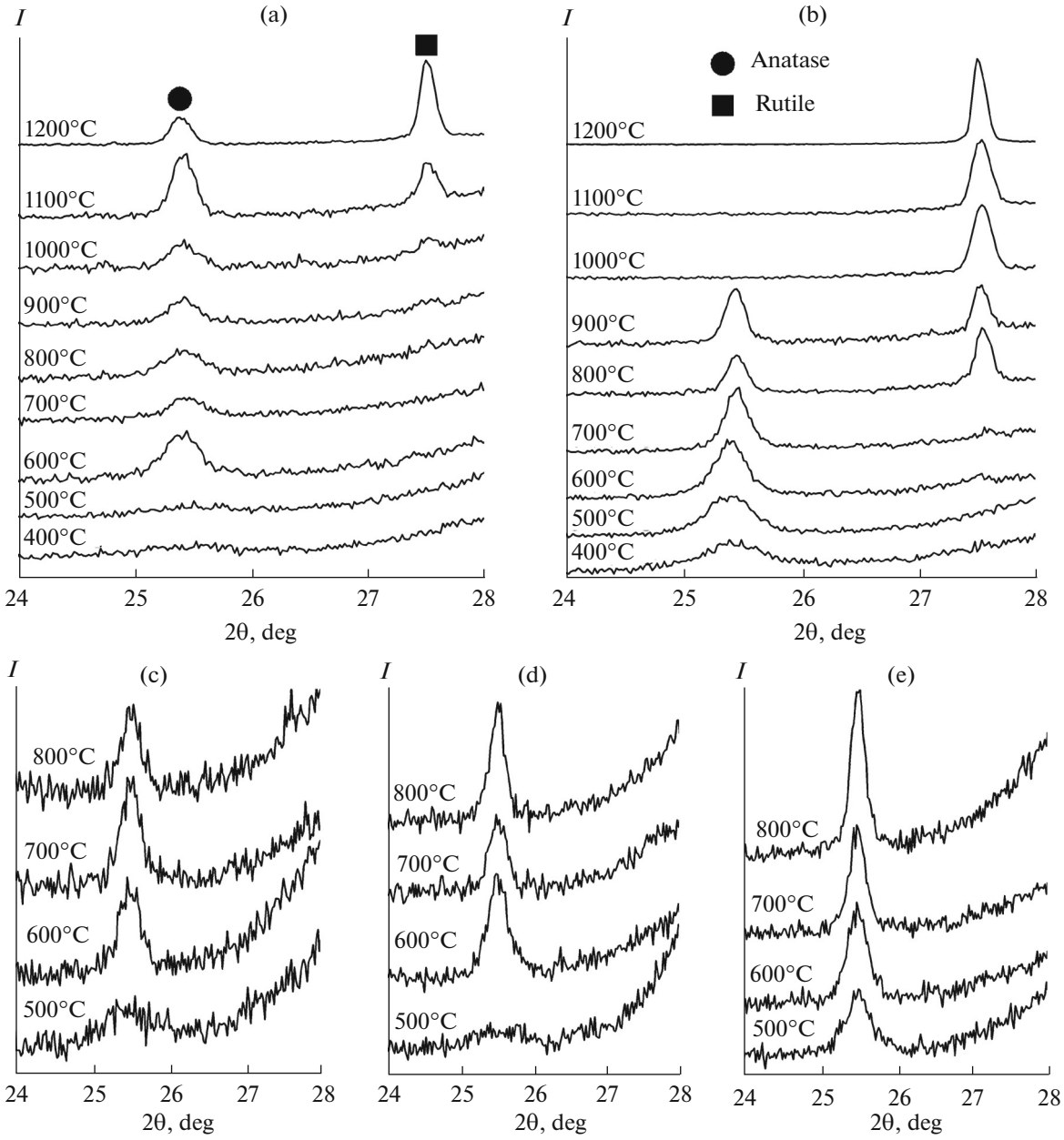

Fig. 2. X-ray diffraction patterns of (a, c, d, e) single-layer and (b) double-layer titania thin films prepared at various temperatures and precursor solution viscosities of (a, b) 7.5, (c) 9.0, (d) 10.5, and (e) 12.0 cP.

structure. Primarily, the ratio between the fractions of fine (anatase) particles and coarser (rutile) particles changed. In addition, the substrate surface manifested itself, possibly due to the softening of the near-surface silica layer and a partial incorporation of TiO_2 particles into its bulk.

Thus, the SEM images clearly illustrate a considerable alteration of titania film microstructure upon the anatase–rutile phase transition and show that this process is intensified as the coating thickness increases.

The results of scanning probe microscopy (SPM) shown in Fig. 4 also indicate the formation of nanostructured films that remained in a highly disperse state until 1100°C; at higher temperatures, the fraction of coarser (100–150 nm) edged rutile particles became higher. The surface roughness did not exceed 40 nm in all samples.

The adhesion of oxide films was evaluated by a standard V-notch test. Our prepared nanostructured titania films were found to refer to maximal adhesion classes of the ISO (0) and ASTM (5B) international

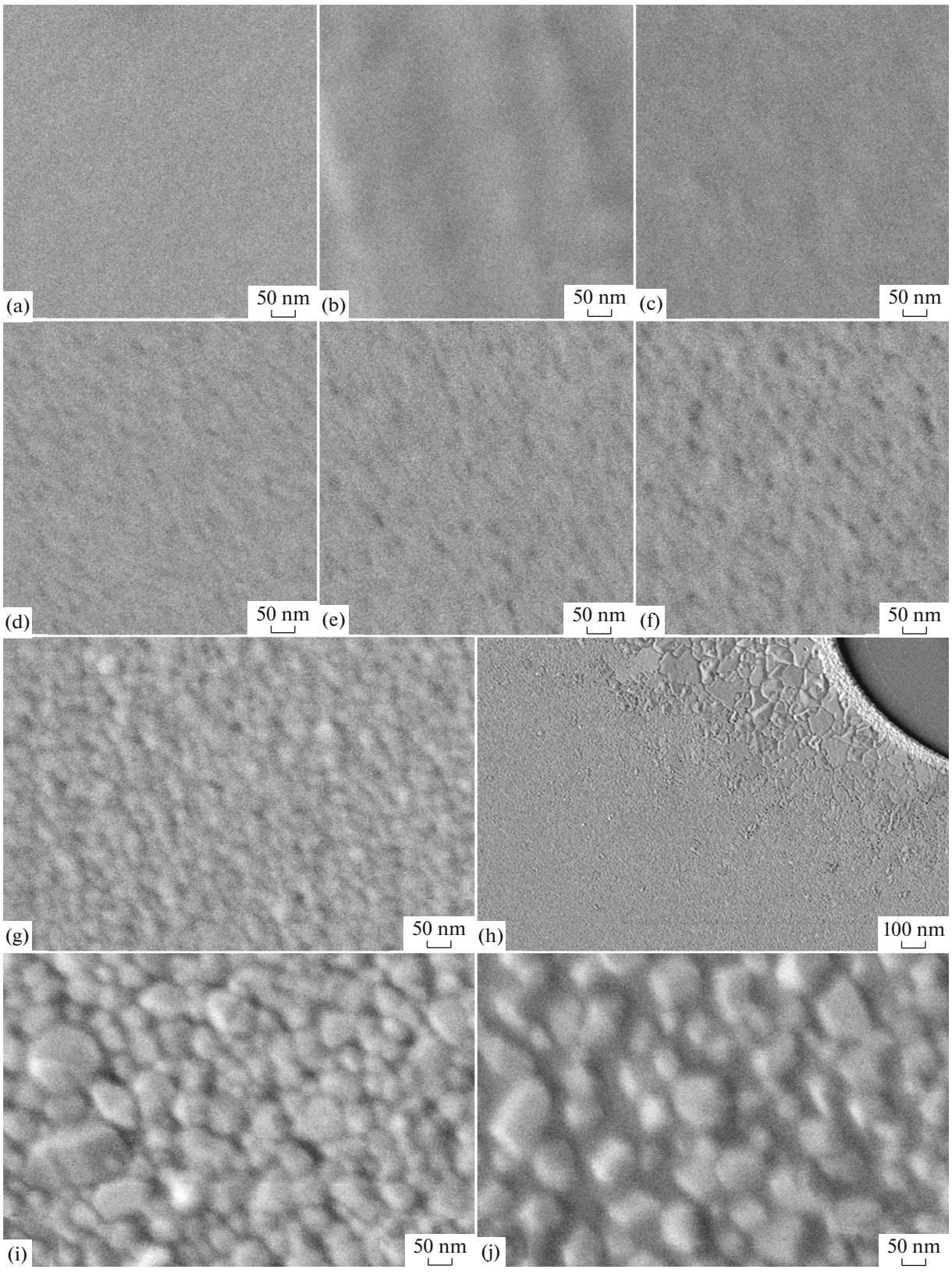

Fig. 3. SEM images of titania thin films prepared at various temperatures: (a) 400, (b) 500, (c) 600, (d) 700, (e) 800, (f) 900, (g, h) 1000, (i) 1100, and (j) 1200°C).

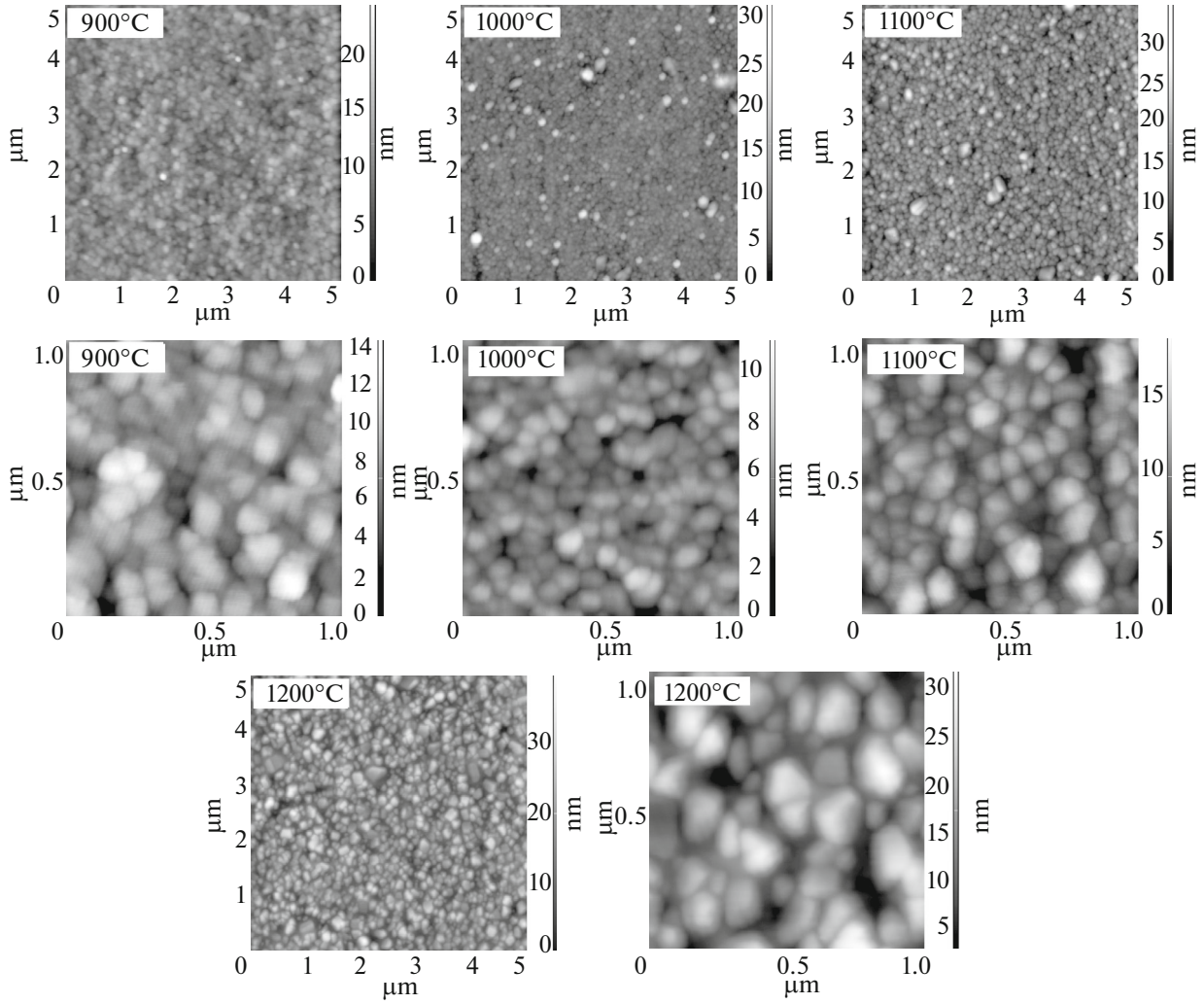

Fig. 4. SPM images of titania thin films prepared at various temperatures.

standards, and the coating technology may be recommended to the manufacturers of relevant structures.

Thus, we have studied the synthesis of hydrolytically active heteroligand complexes of composition $[Ti(OC_4H_9)_{3.61}(O_2C_5H_7)_{0.39}]$ and their hydrolysis and polycondensation, accompanied by the evolution of solution rheology. We have prepared single-layer and double-layer thin nanostructured titania films by dip-coating using precursor solutions of various viscosities, and showed how the coating thickness influences the anatase–rutile phase transition temperature. The higher viscosities of solutions of the complexes during their hydrolysis and polycondensation give rise to the formation of thicker thin oxide films and coarser crystallites upon heat treatment in the same protocol. We also have studied the microstructural evolution of TiO_2 films upon crystallization and the anatase–rutile phase transition. A strong coarsening of particle sizes occurs (by a factor of two to three), which must be taken into account in the manufacture of more efficient thin-film devices for solar cells, photocatalysts, and other electronic and optical components.

ACKNOWLEDGMENTS

This study was supported in part by the Russian Foundation for Basic Research (project no. 15-29-01213 ofi_m) and by the Ministry of Education and Science of the Russian Federation through the Program of activities targeted at improving the competitiveness of the Samara State Aerospace University among the world's leading research and education centers in 2013–2020.

REFERENCES

1. O. Carp, C. L. Huisman, and A. Reller, Prog. Solid State Chem. **32**, 33 (2004).
2. D. Chen, F. Huang, Y.-B. Cheng, et al., Adv. Mater. **21**, 2206 (2009).

3. X. Z. Li, F. B. Li, C. L. Yang, et al., J. Photochem. Photobiol., A **141**, 209 (2001).
4. G. Xingtao and E. W. Israel, Catal. Today **51**, 233 (1999).
5. J. G. Yu, J. C. Yu, M. K. P. Leung, et al., J. Catal. **217** (1), 69 (2003).
6. H. Choi, E. Stathatos, and D. D. Dionysiou, Appl. Catal. B **63**, 60 (2006).
7. J. C. Yu, X. Wang, and X. Fu, Chem. Mater. **16**, 1523 (2004).
8. R. Dholam, N. Patel, M. Adami, et al., Int. J. Hydrogen En. **34**, 5337 (2009).
9. A. Mills, G. Hill, S. Bhopal, et al., J. Photochem. Photobiol., A **160**, 185 (2003).
10. D. Li and Y. Xia, Nano Lett. **4**, 933 (2004).
11. N. T. Kuznetsov, V. G. Sevast'yanov, E. P. Simonenko, et al., RU Pat. No. 2407705 (2010).
12. N. P. Simonenko, V. A. Nikolaev, E. P. Simonenko, et al., Russ. J. Inorg. Chem. **61**, 929 (2016). doi 10.1134/S0036023616080167
13. V. G. Sevast'yanov, E. P. Simonenko, N. P. Simonenko, et al., Russ. J. Inorg. Chem. **57**, 307 (2012). doi 10.1134/S0036023612030278
14. E. P. Simonenko, N. P. Simonenko, V. G. Sevast'yanov, et al., Russ. J. Inorg. Chem. **57**, 1521 (2012). doi 10.1134/S0036023612120194
15. N. T. Kuznetsov, V. G. Sevast'yanov, E. P. Simonenko, et al., RU Pat. No. 2521643 (2014).
16. N. P. Simonenko, E. P. Simonenko, V. G. Sevastyanov, et al., Russ. J. Inorg. Chem. **60**, 795 (2015). doi 10.1134/S0036023615070153
17. N. P. Simonenko, E. P. Simonenko, V. G. Sevastyanov, et al., Russ. J. Inorg. Chem. **61**, 667 (2016). doi 10.1134/S003602361606019X
18. N. P. Simonenko, E. P. Simonenko, Sevastyanov V.G., et al., Russ. J. Inorg. Chem. **61**, 805 (2016). doi 10.1134/S0036023616070184
19. N. P. Simonenko, E. P. Simonenko, V. G. Sevast'yanov, et al., Yadernaya Fiz. Inzh. **5**, 331 (2014).
20. E. P. Simonenko, N. P. Simonenko, V. G. Sevastyanov, et al., Compos. Nanostruct., No. **4**, 52 (2011).
21. Sevastyanov V.G., E. P. Simonenko, N. A. Ignatov, et al., Russ. J. Inorg. Chem. **56**, 661 (2011). doi 10.1134/S0036023611050214
22. E. P. Simonenko, Ignatov N.A., N. P. Simonenko, et al., Russ. J. Inorg. Chem. **56**, 1681 (2011). doi 10.1134/S0036023611110258
23. N. T. Kuznetsov, V. G. Sevastyanov, E. P. Simonenko, et al., RU Patent No. 2333888 (2008).

Translated by O. Fedorova